RESEARCH ARTICLE
doi: 10.2306/scienceasia1513-1874.2025.009

ScienceAsia 51 (1): 2025: ID 2025009: **1–6**

Synthesis and characterization of nutrient fortifier zinc citrate

Zhifu Wu[a,b,c], **Guiquan Guo**[d,*]

[a] School of Pharmacy, Guilin Medical University, Guilin 541199 China
[b] Guangxi Key Laboratory of Drug Molecular Discovery and Optimization, Guilin 541199 China
[c] Engineering Research Center for Drug Molecular Screening and Drug Evaluation in Guangxi Zhuang Autonomous Region, Guilin 541199 China
[d] School of Chemical Engineering and Biotechnology, Xingtai University, Xingtai 054001 China

*Corresponding author, e-mail: guoguiquan1979@163.com

Received 4 Oct 2023, Accepted 2 Dec 2024
Available online 15 Feb 2025

ABSTRACT: Zinc citrate was synthesized using citric acid and zinc hydroxide as raw materials in a high-pressure reactor. The yield, purity, molecular structure, crystal state, and morphology of the product were analyzed using titration, thermogravimetric analysis, FT-IR spectroscopy, X-ray diffraction, and scanning electron microscopy, respectively. The results showed that the morphology of the product consisted of microspheres with nanosheets on the surface. The chemical composition indicated that the product had zinc-oxygen bonds and contained 10 molecules of crystal water. This zinc citrate was synthesized using the hydrothermal method.

KEYWORDS: zinc citrate, hydrothermal method, spherical particles, crystal water

INTRODUCTION

Zinc exists in almost all types of organisms, plays an important role in the physiological activities of humans and animals, and is also an indispensable nutrient for plant growth and development [1–4]. Zinc is one of the essential trace elements in the human body, widely existing in all parts of the human body, and ranks second only to iron in the content of trace elements in the human body. It is involved in the growth and development of the human body, immunity, endocrine, reproductive genetics and other processes, and has important regulatory functions on human health. It is known as "the source of wisdom" and "the flower of life" [5]. The human genome encodes more than 2,800–3,000 Zn proteins, which make up about 10% of the human proteome. Zinc is the reaction center of more than 300 metabolic enzymes, and more than 50 different types of functions require zinc [6]. Zinc supplements can be divided into 2 categories: inorganic and organic zinc supplements. Common inorganic zinc supplements are zinc sulfate, zinc chloride, etc., which are inexpensive, but the absorption rate is low and can cause some irritation. Common organic zinc supplements are zinc gluconate, zinc lactate, zinc citrate, zinc picolinate, and zinc amino acid chelate, of which their bioavailability is high, and they cause less stomach irritation. The most common organic zinc supplements on the market are zinc gluconate and zinc citrate, with bioavailability of 60.9% and 61.3%, respectively. Although zinc citrate and zinc gluconate have similar effects on zinc supplementation, they may also be effective in treating diarrhea [7]. Zinc citrate has some unique effects. For example, it is better than zinc gluconate when choosing suitable drugs to supplement zinc for diabetic patients. On the one hand, zinc citrate does not antagonize iron supplements. On the other hand, the stability of zinc citrate is also higher than that of other commonly used organic zinc supplements such as zinc gluconate and zinc lactate. Zinc gluconate, zinc lactate, and zinc citrate will begin thermal decomposition at 150, 190, and 280 °C, respectively. In addition, when used as a food fortification, the economic benefits of using zinc citrate can be twice that of zinc lactate and 6 times that of zinc gluconate. Zinc citrate can not only be used to enhance the body's immunity and the human digestive function and promote wound healing but also can be used to assist the treatment of developmental delays, anorexia, dermatitis, and other diseases. It can also be used to give zinc supplements to diabetic patients. Because zinc citrate does not antagonize iron, zinc citrate can be used together with iron. It can also be used as a component of toothpaste to prevent and treat dental plaque, relieve gingivitis, and prevent dental calculus [8]. Additionally, it can also be used as a new oral liquid gargle to inhibit tooth stains and effectively inhibit the deposit of exogenous pigments on teeth [9]. In the food industry, zinc citrate can be used as a good zinc supplement [10] in dairy products, as zinc citrate is the only form of zinc present in breast milk [11].

In this experiment, zinc citrate with high purity was prepared by hydrothermal reaction method with zinc hydroxide and citric acid as raw materials. To characterize the product, molecular structure, particle size, purity, and crystal state were analyzed by FT-IR spectrophotometer, scanning electron microscope, thermogravimetric analyzer, and X-ray diffractometer, respectively.

MATERIALS AND METHODS

Reagents and instruments

Citric acid ($C_6H_8O_7$), $Zn(NO_3)_2 \cdot 6H_2O$, NaOH, $K_4Fe(CN)_6$, HCl, $HgSO_4$, H_2SO_4, $KMnO_4$, NH_3-NH_4Cl buffer, EDTA, all of the reagents described above were analytically pure (AR) and purchased from Sinopharm Chemical Reagents Co., Ltd. in Shanghai, China.

The FT-IR spectrum of the synthesized sample was measured by Fourier transform infrared spectrometer (NEXUS 870, Thermo Nicolet Corporation, Madison, USA). The thermal property of the synthesized sample was characterized by thermogravimetric analysis (STA 449 F5, NETZSCH Group, Bavaria, Germany). The morphology of the sample was carried out by scanning electron microscopy (Regulus 8100, Hitachi Corporation, Tokyo, Japan). Powder X-ray diffraction (XRD) pattern of the as-prepared sample was investigated on an XRD-6100 (Shimadzu Corporation, Kyoto, Japan) diffractometer.

Experimental procedure

A 11.90 g of $Zn(NO_3)_2 \cdot 6H_2O$ (40 mmol) was weighed, dissolved in water, and made up to 250 ml. Then, 3.20 g of NaOH (80 mmol) was weighed, dissolved in water, and made up to 250 ml. While stirring, the NaOH solution was added to the $Zn(NO_3)_2$ solution drop by drop, with the temperature controlled below 30 °C. After dropping, it was stirred for 2 h and then aged in a constant temperature water bath at 25 °C for 5 days. Finally, the precipitate was filtered out and air-dried to obtain $Zn(OH)_2$ [12].

The obtained $Zn(OH)_2$ (1.81 g) and 5.9 g/l citric acid aqueous solution (6 ml) were heated at 120 °C for 5 h in a stainless steel reactor with a polytetrafluoroethylene (PTFE) liner, let cool to room temperature naturally, and filtered to obtain a product.

Testing of products

Inspection using the inspection method of food safety national standard GB1903.49-2020

A 0.2 g of the product was weighed, dissolved in 20 ml of water, and then 2 ml of newly prepared potassium ferrocyanide solution was added to it, resulting in white precipitate. The precipitate was filtered, and a hydrochloric acid solution was added to it. The precipitate was insoluble, which proved to be zinc salt. A few drops of sulfuric acid solution were added to 5 ml of 2 g/l product solution, and the solution was heated to boiling. Then, a few drops of potassium permanganate solution were added and shaken, and the purple color disappeared. Then, a mercury sulfate solution was added to form white precipitate; it can be proved to be citrate [13]. The above 2 experiments prove that the synthesized product is both zinc salt and citrate, so it can be inferred that the product is zinc citrate.

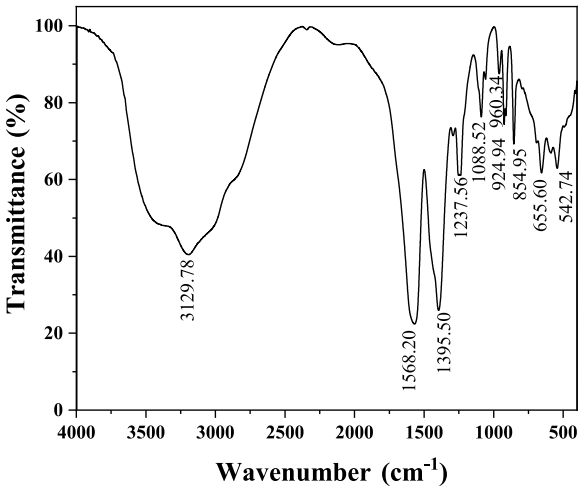

Fig. 1 FT-IR spectrum of the product.

Content determination

The dried product was about 0.2 g, and 20 ml of distilled water and 10 ml of ammonia-ammonium chloride buffer solution, pH 10.0 were added and shaken until dissolved. Then, a little chromium black T indicator was added and titrated with 0.05 mol/l EDTA until the solution changed from purple to pure blue. At last, 20.6 ml of 0.05 mol/l EDTA titrant was consumed, and the content of zinc citrate in the sample was determined to be 98.6%. It is in line with the standard content of zinc citrate in the second part of Chinese Pharmacopoeia and national standards [14].

RESULTS AND DISCUSSION

Infrared spectrum (IR)

Fig. 1 shows the FT-IR spectrum of the prepared product. The structure of its characteristic absorption peaks is as follows: the peak appearing at 3129.78 cm^{-1} of the FT-IR spectrum of the product is the absorption peak of O—H stretching vibration in crystalline water. The peaks at 1568.20 cm^{-1} and 1395.50 cm^{-1} are the antisymmetric stretching vibration and symmetric stretching vibration of COO^- in carboxylate, respectively. The peaks at 1237.56 cm^{-1} and 1088.52 cm^{-1} are the C—O stretching vibration absorption peak of carboxylate and alcohol, respectively. [15, 16]. The peaks at 960.34 cm^{-1}, 924.94 cm^{-1}, and 854.95 cm^{-1} refer to the stretching vibration absorption peak of C—H, and the peaks at 655.60 cm^{-1} and 542.74 cm^{-1} refer to the stretching vibration absorption peak of Zn—O [17]. The structure of the main absorption peak in the FT-IR spectrum in the figure is consistent with that of zinc citrate. Compared with citric acid, the FT-IR spectrum of the product is mainly shifted compared with the bimodal feature of COO^- in citric acid. The shift of bimodal characteristics and the

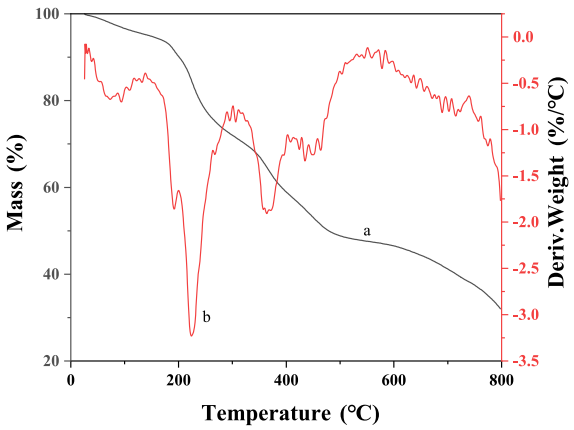

Fig. 2 TG-DTG curves of zinc citrate (a: TG and b: DTG).

disappearance of characteristic bands in the IR spectra of citric acid indicate that —COOH reacts with Zn^{2+} to form carboxylate.

Thermogravimetric analysis (TGA)

In order to evaluate the thermal stability and crystal water content of the product, we carried out thermogravimetric analysis. Fig. 2 shows the TG-DTG curve of zinc citrate. With the increase of heating temperature, the mass of zinc citrate changes significantly in 3 stages. The first stage is when the temperature increases from 25 to 200 °C, the curve a shows that the sample mass is reduced by 4.80%, and it is speculated that the adsorbed water is lost at this temperature. This is shown as a downward endothermic valley on the corresponding differential thermogravimetric curve b, which is consistent with the theory of adsorbed water evaporation. The second stage is when the temperature rises from 200 to 500 °C, the curve a shows that the mass of the sample is reduced by 23.25%, and the corresponding differential thermogravimetric curve b also shows a downward endothermic valley. The literature indicates that the structural water decomposition temperature of zinc citrate is about 365 °C. The weight loss at this stage is equivalent to 10 crystal water molecules, which is consistent with the theoretical calculation value of 23.90% [18]. Therefore, it is inferred that the sample contains 10 crystal water molecules. The third stage is when the temperature increases from 500 to 800 °C, the curve a shows that the sample mass is reduced by 40.00%, corresponding to the sample decomposition stage. Curve b shows an upward broad peak, indicating that it is an exothermic reaction. The product decomposes to produce carbon dioxide and water, and the water at this time is structural water. According to theoretical calculation, the mass loss of zinc citrate due to its decomposition into water and carbon dioxide should be 43.10%. After the sample is completely decomposed, the remaining product zinc oxide should theoretically account for 32.37% of the total mass of the sample. The final experimental results show that the mass of the remaining solid matter accounts for 31.95% of the total mass of the original sample, and the error between the actual value and the theoretical value is very small.

Scanning electron microscope (SEM)

Fig. 3 shows the SEM images of the synthesized product, and the product particles are spherical distributed at low magnification. From Fig. 3a, the product consists of spherical particles. Fig. 3a is an SEM image of the product at 100 times magnification, at which it can be seen that the particles are spherical, and the maximum grain size is 140 µm, the minimum is 5 µm, and the average particle size is 62.5 µm. Fig. 3b is an SEM image of a single particle at 1,000 times magnification with a diameter of 36.6 µm. Fig. 3c shows an SEM image at 5,000 times magnification of the product particles with a shown particle diameter of 13 µm. Some debris particles are attached to the spherical particle surface. Fig. 3d shows an SEM image of the product particles magnified by 5,000 times, which more obviously shows the characteristics of the sheet particles on the spherical surface. Fig. 3e shows the selected area electron diffraction energy spectrum of the product spherical particles. Because the energy spectrometer cannot detect the H element, the distribution of C, O, and Zn can be shown in the figure. To further understand the morphological characteristics of these attached particles, Fig. 4 specifically characterizes these sheet particles, as shown below.

The morphology of the debris particles attached to the spherical particles can be seen in Fig. 4. According to Fig. 4c, an approximately triangular debris can be detected, and the lengths of 3 sides are about 2.3, 2.2, and 1.3 µm. It can be estimated from Fig. 4f that the thickness of debris particles is around 30 nm. In Fig. 4a, the debris particles vary in size, and the smaller debris particles are attached to larger debris particles. In Fig. 4b, the debris particles are also uneven, and the smaller debris particles appear to be formed by splitting from a larger debris particle. In Fig. 4c, the states of the debris particles are not all extended, and some of the debris particles have a tendency to shrink. In Fig. 4d, the edges and corners of the debris particles are more rounded. It can be clearly seen in Fig. 4e that there are 2 different phenomena of debris particles. One spreads out to become a new, smaller debris particle, while the other crumbles up to become the irregularly shaped geometry shown in Fig. 4a. In Fig. 4f, the debris particle trend and some of the particles began to crumple together after splitting. Fig. 4g is the selected area electron diffraction energy spectrum of the debris particles. Because H element cannot be detected by the energy spectrometer, only

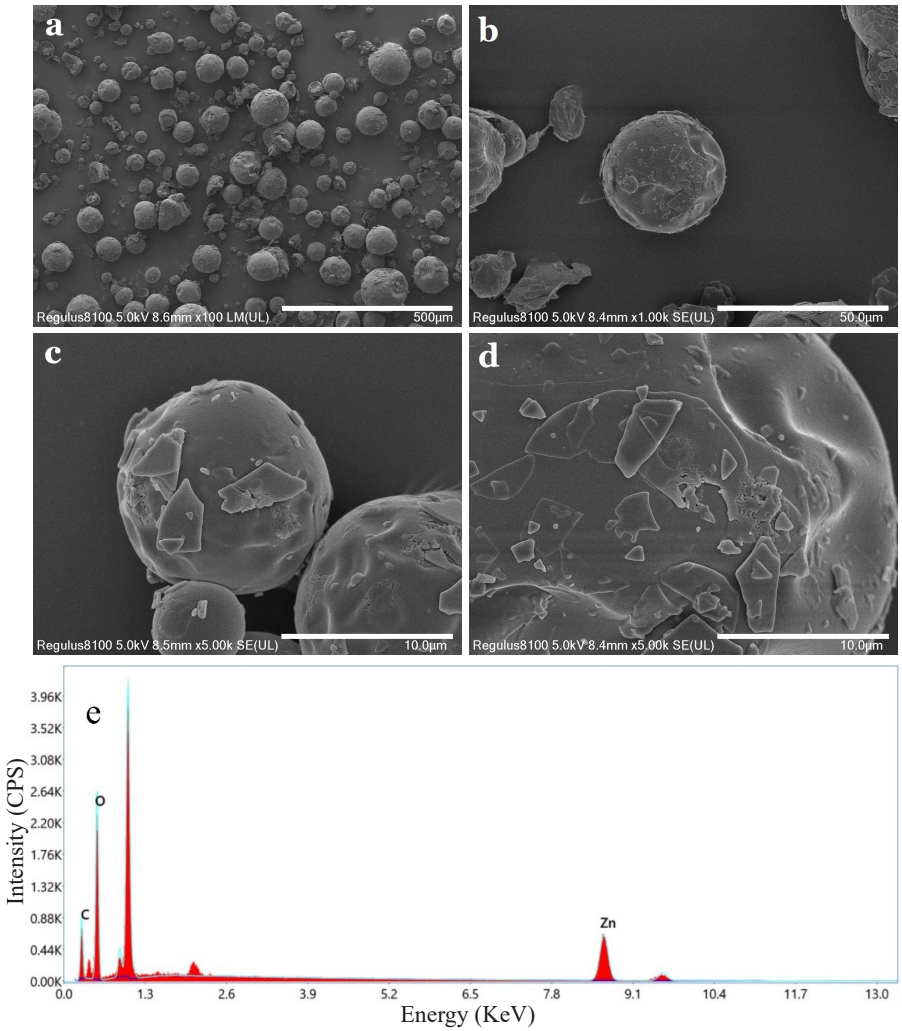

Fig. 3 SEM images (a: 100 times, b: 1,000 times, and c–d: 5,000 times) and (e) selected area electron diffraction energy spectrum of the synthesized product.

the distribution of C, O, and Zn is shown in the figure. They are consistent with the elements contained in the spherical selection.

The reasons for the formation of spherical crystals may be as follows: first, the inorganic matter forms a crystal nucleus, which is surrounded by organic matter. Under the action of the Coulomb field of the nucleus, the nanocrystals embedded in organic matter are automatically arranged in a radial manner to produce spherical structural units [19]. In this experiment, zinc hydroxide first forms charged nuclei. Another part of the citric acid wraps up into a bundle of dipoles, which clumps together with the charged nucleus to form a spherical particle. Through the analysis of SEM images, it can be concluded that zinc citrate chelates with spherical particles can be prepared by the hydrothermal method, and the debris particles can reach nanometer level. Spherical particles are more stable and fluid than particles of other shapes. Therefore, zinc citrate chelates with good quality can be synthesized by hydrothermal method [20].

X-ray diffraction (XRD)

Fig. 5 shows the X-ray diffraction spectrum of the prepared product; the strongest peaks in 2θ of 9.42°, 27.74°, and 40.04° are consistent with the literature report binding chemical analysis, which shows that the synthesized product is hydrate zinc citrate chelate [21, 22].

The thickness of the crystal sheet can be calculated using the formula of $D = \frac{K\lambda}{B\cos\theta}$, where D is the average thickness (nm) of the grain perpendicular to the direction of the crystal surface and K is Scherrer constant. If B is the half height width of the diffraction peak of the measured sample, radian (rad), K = 0.89;

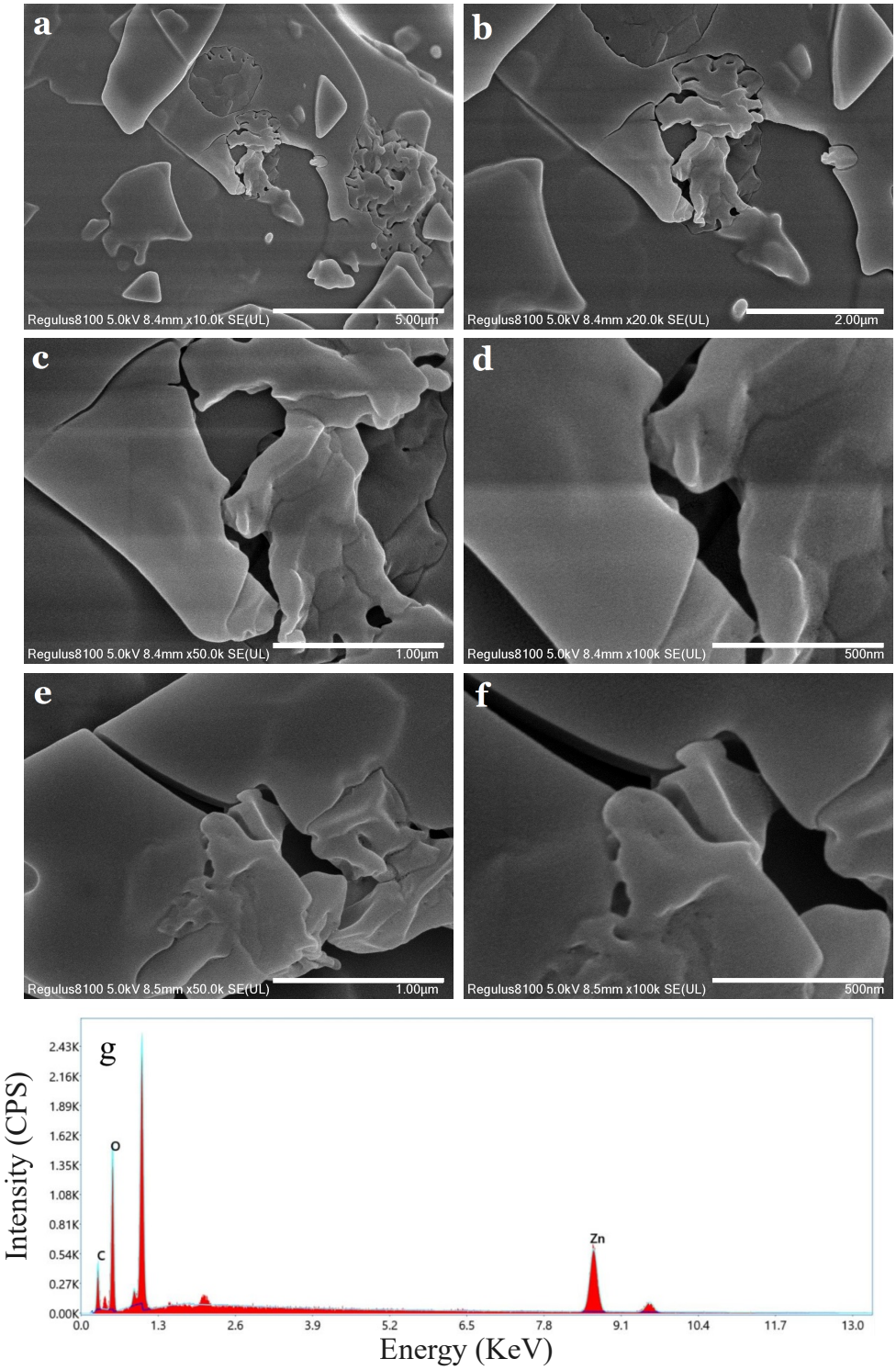

Fig. 4 SEM images (a: 10,000 times, b: 20,000 times, c and e: 50,000 times, and d and f: 100,000 times) and (g) selected area electron diffraction energy spectrum of debris particles attached to the surface.

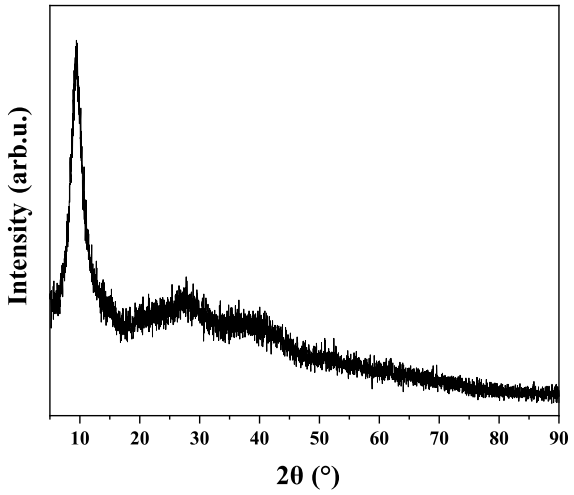

Fig. 5 XRD patterns of the obtained product.

if B is the integral width of the diffraction peak, K = 1; θ is the Bragg diffraction angle (in degrees); λ is the X-ray wavelength which equals to 0.154056 nm. Therefore,

$$D = \frac{K\lambda}{B\cos\theta} = \frac{0.89 \times 0.154056}{\frac{2.207\times3.14}{180} \times \cos(4.63275)} = 3.58 \text{ nm}.$$

CONCLUSION

Zinc citrate hydrate was synthesized by the hydrothermal reaction of zinc hydroxide and citric acid aqueous solution with a yield of 97.8%. Through inspection, it was found that the product met the quality standard of the Chinese Pharmacopoeia. SEM images showed that most of the synthesized product particles were spherical crystals attached to nanoparticles.

Acknowledgements: The authors are grateful for the financial support of the Xingtai Science and Technology Plan Project (2023ZZ076).

REFERENCES

1. Karunasinghe N (2022) Zinc in prostate health and disease. *Biomedicines* **10**, 3206–3208.
2. Gowalock DW, Mahan DC, Samuel RS (2016) Evaluating dietary adjustment and collection times for total tract digestibility of Ca, P, and the essential microminerals with grower swine. *J Anim Sci* **94**, 3264–3270.
3. Kasprzyk A, Kilar J, Chwil S (2020) Content of selected macro- and micro-elements in the liver of free-living wild boars from agricultural areas and health risks associated with consumption of liver. *Animals* **10**, 1519–1536.
4. Laenoi S, Prom-u-thai C, Dellc B, Rerkasem B (2015) Iron and zinc variation along the grain length of different Thai rice varieties. *ScienceAsia* **41**, 386–391.
5. Tian ZM, Cui YY, Deng D (2022) Physiological function of zinc and its application in pig breeding. *Chin J Anim Husb Vet Med* **49**, 4228–4238.
6. Cheng LN, Li DR (1995) Study on synthesis technology of food additive zinc citrate. *J Zhengzhou Grain U* **11**, 41–45.
7. Rita W, Fabian T, Christophe Z (2014) Zinc absorption by young adults from supplemental zinc citrate is comparable with that from zinc gluconate and higher than from zinc oxide. *J Nutr* **144**, 132–136.
8. Ding GJ, Cheng JP, Yan M (2020) Progress in the application of zinc citrate in oral care products. *Oral Care Prod Ind* **30**, 6–10.
9. Li N, Cui XM, Li JN (2018) Preliminary observation on the inhibitory effect of dextran, sodium lauryl sulfate and zinc citrate on dental plaque attachment. *China Pres Drugs* **16**, 160–161.
10. Li WP, Meng TL (1995) Zinc citrate and its application in dairy industry. *Sci Technol Food Ind* **11**, 56–58.
11. Jiang JZ, Tang YG, Peng XG (1997) Synthesis and structure analysis of zinc citrate. *Chem React Eng Technol* **1**, 73–77.
12. Wu ZF, Li SJ (2012) Infrared spectroscopic characteristics of zinc hydroxide and zinc oxide. *Spectrosc Lab* **29**, 2172–2175.
13. State Administration for Market Regulation (2020) *Food Safety National Standard GB1903.49-2020*. National Health Commission of the People's Republic of China.
14. National Pharmacopoeia Commission (2020) *Chinese Pharmacopoeia*, China Medical Science and Technology Press, Beijing, China.
15. Bichara LC, Lanús HE, Brandán SA (2014) Stabilities of aqueous solutions of sucrose containing ascorbic and citric acids by using FTIR spectroscopy and physicochemical studies. *J Mol Liq* **200**, 448–459.
16. Pehlivanoglu SA, Polat O (2023) Exploring the structural and optical properties of Ir-doped ZnO thin films. *Opt Mater* **143**, 114179.
17. Winiarski J, Tylus W, Winiarska K, Szczygieł I, Szczygieł B (2018) XPS and FT-IR characterization of selected synthetic corrosion products of zinc expected in neutral environment containing chloride ions. *J Spectrosc* **2018**, 2079278.
18. Tsioptsias C, Panagiotou A, Mitlianga P (2024) Thermal behavior and infrared absorbance bands of citric acid. *Appl Sci* **14**, 8406.
19. Zhou WZ (2019) Structure and formation mechanism of spherulite. *J Fudan U (Nat Sci Ed)* **61**, 653661–653669.
20. Moeinipour A, Afkhami A, Madrakian T (2024) Hydrogen-bonded organic frameworks as a carrier for nanodrugs with host-guest interaction for smart wound dressing applications. *ChemistrySelect* **9**, e202404417.
21. Wang H, Han XZ, Huang HD (2020) Preparation and characterization of zinc citrate chelate. *Phos Comp Fert* **35**, 33–35.
22. Todica M, Muresan-Pop M, Niculaescu C, Constantiniuc M (2020) XRD and FTIR investigation of the structural changes of the human tooth induced by citric acid. *Rom J Phys* **65**, 706.